Journal of Structural Chemistry. Vol. 53, No. 4, pp. 740-747, 2012

Devoted to the Jubilee of Academician F. A. Kuznetsov

CRYSTAL STRUCTURES OF 1,1,1-TRIFLUORO-4-HYDROXY-4-PHENYL-BUT-3-EN-2-ONE, 2,2,6,6-TETRAMETHYL-3-HYDROXY-HEPT-3-EN-5-ONE, 2,2,6,6- TETRAMETHYL-3-METHYLAMINO-HEPT-3-EN-5-ONE AND A STUDY OF THE ABILITY OF THESE LIGANDS TO COMPLEX FORMATION WITH METALS

© **P. A. Stabnikov, L. G. Bulusheva, N. I. Alferova, A. I. Smolentsev, I. A. Korol'kov, N. V. Pervukhina, and I. A. Baidina**

UDC 548.737:541.49

Crystal structures are determined (Bruker Nonius X8 Apex, 4K CCD-detector, λMoK_α, graphite monochromator, T 150 K and 293 K) for two β-diketones $F_3CC(O)CH_2C(O)Ph$ (**1**) (space group $P2_1/c$, a = 7.0713(3) Å, b = 11.5190(6) Å, c = 11.3602(6) Å, β = 99.405(2)°, V = 912.90(8) Å^3, Z = 4), $(CH_3)_3CC(O)CH_2C(O)C(CH_3)_3$ (**2**) (space group $Pbca$, a = 11.5536(8) Å, b = 11.5796(10) Å, c = 17.2523(13) Å, V = 2308.1(3) Å^3, Z = 8) and a ketoimine $(CH_3)_3CC(NCH_3)CH_2C(O)C(CH_3)_3$ (**3**) (space group $I4_1/a$, a = 18.7687(6) Å, b = 18.7687(6) Å, c = 14.5182(6) Å, V = 5114.2(3) Å^3, Z = 16). All structures are molecular and comprise isolated molecules joined by van der Walls interactions. The substitution energy of a Na atom for a hydrogen atom in free ligands is calculated by the hybrid B3LYP quantum chemical method. A successful preparation of Na(I) chelates with ligands **1**, **2** and failed attempts to prepare a complex with ligand **3** are in accordance with the calculations. Geometrical simulation of a copper(II) complex with ligand **3** reveals the overlap of CH_3 groups which hinders the complexation.

Keywords: β-diketones, crystal structure, molecular packing, chelate formation.

Metal complexes of β-diketones and their nitrogen-substituted analogs are volatile, i.e., can be transferred into the gas phase by moderate heating without decomposing the molecules. Due to this property, metal β-diketonates are widely applied to obtain metal and oxide coatings (MO CVD [1, 2]). Extended applications facilitated a comprehensive investigation of these metal complexes, including their structures in the crystalline state, as indicated by CCDC (Cambridge Crystallographic Data Centre). However, while metal complexes are well represented in CCDC, the structure of the starting ligands is less studied. Data on the structures of the ligands are necessary to understand both chemical transformations occurring during the complex formation and processes of thermal destruction of the compounds. The structures of several

A. V. Nikolaev Institute of Inorganic Chemistry, Siberian Division, Russian Academy of Sciences, Novosibirsk; stabnik@niic.nsc.ru. Translated from *Zhurnal Strukturnoi Khimii*, Vol. 53, No. 4, pp. 751-757, July-August, 2012. Original article submitted July 12, 2011; revised November 30, 2011.

 0022-4766/12/5304-0740

TABLE 1. Structural Data for β-Diketones Studied

Ligand, reference	CSD refcode	Year	Space group, *Z*	*a*	*b*, β	*c*	*R*	*T*, K
Haa [3]	LIWPIQ	1998	*Pnma*, 4	8.396	15.984	4.066	4.81	110
	LOWPIQ01	1998	*Pnma*, 4	8.463	16.031	4.146	6.45	210
$[Bi(dpm)_3]_2$·Hdpm [4]	YIJYEV	1993	*C*2/*c*, 8	43.396	20.455, 104.27	18.499	3.85	207
NC-dpm [5]	HAKTIX	2004	$P2_1/c$, 4	9.957	20.405, 91.30	5.980	5.3	100
I-dpm [6]	KUGPUX	1992	$P2_1/c$, 4	9.188	14.229, 104.74	10.628	3.9	250
Hdbm [7]	DBEZLM05	1997	*Pbca*, 8	8.749	10.840	24.427	6.49	283

β-diketones present in CCDC are given in Table 1 [3-7]. A structural examination has not been carried out for 1,1,1-trifluoro-4-hydroxy-4-phenyl-but-3-en-2-one (**Hbtf**, **1**), 2,2,6,6-tetramethyl-3-hydroxy-hept-3-en-5-one (**Hdpm**, **2**), and 2,2,6,6-tetramethyl-3-methylamino-hept-3-en-5-one (**Hmi-dpm**, **3**). This study reports the investigation of the crystal structures of these ligands, quantum-chemical calculations, and modeling of chelate formation.

EXPERIMENTAL

The Hbtf and Hdpm ligands were purchased from Merck and Dalsib. Hmi-dpm was prepared by amination of Hdpm with gaseous NH_2CH_3 in the presence of $TiCl_4$, as described for the synthesis of 2,2,6,6-tetramethyl-3-amino-3-hepten-5-one (**Hi-dpm**, **4**) in [8]. Hmi-dpm is white powder insoluble in water and soluble in organic solvents. Ligand melting points (hotplate microscope, °C): 148 (**1**), 19 (**2**), 40 (**3**). C, H, N, F analytical data were obtained on Carlo-Erba 1106 (Italy). For **1** found, %: C 55.5, H 3.2, F 26.4. For $C_7H_7O_2F_3$ calculated, %: C 55.6, H 3.3, F 26.4. For **2** found, %: C 71.8, H 10.8. For $C_{11}H_{20}O_2$ calculated, %: C 71.7, H 10.9. For **3** found, %: C 73.2, H 11.6, N 7.2. For $C_{12}H_{23}ON$ calculated, %: C 73.0, H 11.8, N 7.1.

IR spectra of the samples were recorded on a Fourier SCIMITAR FTS 2000 spectrophotometer within the range 375-4000 cm^{-1} in KBr pellets. The resulting spectra are shown in Fig. 1. Selected vibrations for these ligands are:

1 (cm^{-1}) ν_{O-H} 3493, 3400; ν_{C-H} 3122, 3078; $\nu_{C=O}$ 1617, 1580; ν_{C-F} 1312, 1289, 1255; δ_{C-F} 773, 900.

2 (cm^{-1}) ν_{O-H} 3445; ν_{C-H} 2967, 2902, 2872; $\nu_{C=O}$ 1605.

3 (cm^{-1}) ν_{O-H} 3406; ν_{N-H} 3210; ν_{C-H} 2964, 2901, 2875; $\nu_{C=O}$ 1604, 1572; δ_{N-H} 1524; ν_{C-N} 1203.

4 (cm^{-1}) ν_{N-H} 3406, 3347, 3175; ν_{C-H} 2967, 2907, 2868; $\nu_{C=O}$ 1633, 1596; δ_{N-H} 1525; ν_{C-N} 1216.

Interaction of the ligands with sodium metal. The experiments were carried out in dry dioxane. Four test tubes were loaded with 0.013 g of Na, ~5 ml of dioxane and ~ 0.2 g of Hbtf, Hdpm, Hi-dpm, and Hmi-dpm (double excess of the ligand). Hydrogen evolution was noticed in the tube with Hbtf at room temperature. On heating to 40°C it became observable also in the tube with Hdpm. On further heating to 80°C the dissolution of sodium accelerated in these tubes, and the reaction of Na with Hi-dpm became recognizable. No reaction between Na and Hmi-dpm was observed at this temperature. The heating of the last tube to the dioxane boiling temperature (~101°C) did not result in the evolution of hydrogen. After heating the tubes to 80°C for 1 h they were cooled to room temperature. In the tubes with Hbtf and Hdpm, sodium reacted completely. In the tube with Hi-dpm, sodium was half-dissolved, while in the tube with Hmi-dpm, the weight of sodium did not change.

Interaction of the ligands with $Cu(OH)_2$. Freshly prepared $Cu(OH)_2$ was obtained in a water-acetone mixture (1:1) by the reaction of a copper(II) salt with NaOH. The precipitate of $Cu(OH)_2$ was collected on a filter and washed with acetone. The precipitate was placed in four evaporating dishes, and 0.2 g samples of Hbtf, Hdpm, Hi-dpm, and Hmi-dpm were added to each of them. (Each of the dishes had a ~1.5-fold excess of $Cu(OH)_2$.) The expected reaction was

$$Cu(OH)_2 + 2HL \rightarrow Cu(L)_2 + H_2O.$$

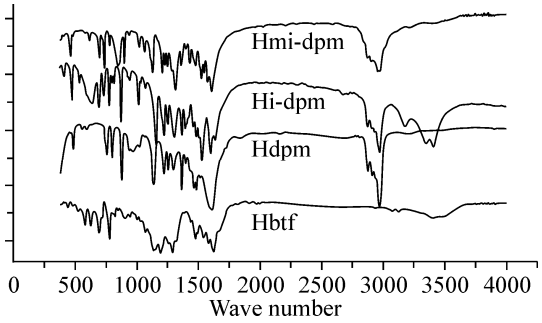

Fig. 1. IR spectra of the ligands.

TABLE 2. Crystal Data and Experimental Details for Compounds **1**, **2**, and **3**

Compound	**1**	**2**	**3**
Formula	$C_{10}H_7F_3O_2$	$C_{11}H_{20}O_2$	$C_{12}H_{23}ON$
Molecular weight	216.2	184.3	197.3
Temperature, K	150(2)	150(2)	293(2)
Wavelength, Å	0.71073	0.71073	0.71073
Crystal system	Monoclinic	Orthorhombic	Tetragonal
Space group	$P2_1/c$	$Pbca$	$I4_1/a$
Unit cell parameters a, b, c, Å; β, deg	7.0713(3), 11.5190(6), 11.3602(6); 99.405(2)	11.5536(8), 11.5796(10), 17.2523(13)	18.7687(6), 18.7687(6), 14.5182(6)
V, Å^3	912.90(8)	2308.1(3)	5114.2(3)
Z	4	8	16
d_x, g/cm^3	1.573	1.061	1.025
μ, mm^{-1}	0.148	0.071	0.064
Crystal size, mm	0.22×0.12×0.06	0.34×0.28×0.22	0.24×0.20×0.22
θ range, deg	2.54-27.57	2.36-26.40	3.07-27.11
I_{hkl} measured	6908	15358	18850
$I_{hkl} > 2\sigma_I$	2103 [R_{int} = 0.0191]	2362 [R_{int} = 0.0257]	2808 [R_{int} = 0.0297]
$GOOF$ on F^2_{hkl}	1.054	1.068	1.061
R ($I > 2\sigma_I$)	R_1 = 0.0344, wR_2 = 0.0936	R_1 = 0.0396, wR_2 = 0.1054	R_1 = 0.0566, wR_2 = 0.1508
R (I_{hkl} msrd.)	R_1 = 0.0439, wR_2 = 0.0985	R_1 = 0.0514, wR_2 = 0.1100	R_1 = 0.0732, wR_2 = 0.1579

Changes in the color of the reaction mixture indicated the formation of $Cu(btf)_2$ and $Cu(dpm)_2$. No reaction was observed between Hi-dpm, Hmi-dpm, and $Cu(OH)_2$. However, in one day, dry residue gave evidence of the formation of $Cu(i\text{-}dpm)_2$, but no reaction was observed for Hmi-dpm.

X-ray crystallography. The unit cell parameters and experimental intensity data were measured at 150 K for $C_{10}H_7F_3O_2$ (**1**), $C_{11}H_{20}O_2$ (**2**) and at 293 K for $C_{12}H_{23}ON$ (**3**) on an automated Bruker Nonius X8 Apex diffractometer equipped with a 4K CCD-detector by the standard method (λMoK_α, graphite monochromator). Semiempirical absorption correction was applied using the intensities of equivalent reflections (SADABS) [9]. The structures were solved by the direct method and refined by full-matrix least squares against F^2 in the anisotropic approximation for non-hydrogen atoms using the SHELX97 package [10]. Hydrogen atoms of the organic ligands were set in geometrical positions and refined in the rigid body approximation. Crystallographic data and experimental details are given in Table 2. Structural data for $C_{10}H_7F_3O_2$ (**1**), $C_{11}H_{20}O_2$ (**2**), and $C_{12}H_{23}ON$ (**3**) have been deposited with CCDC (CCDC 769663, CCDC 755632, CCDC 840627).

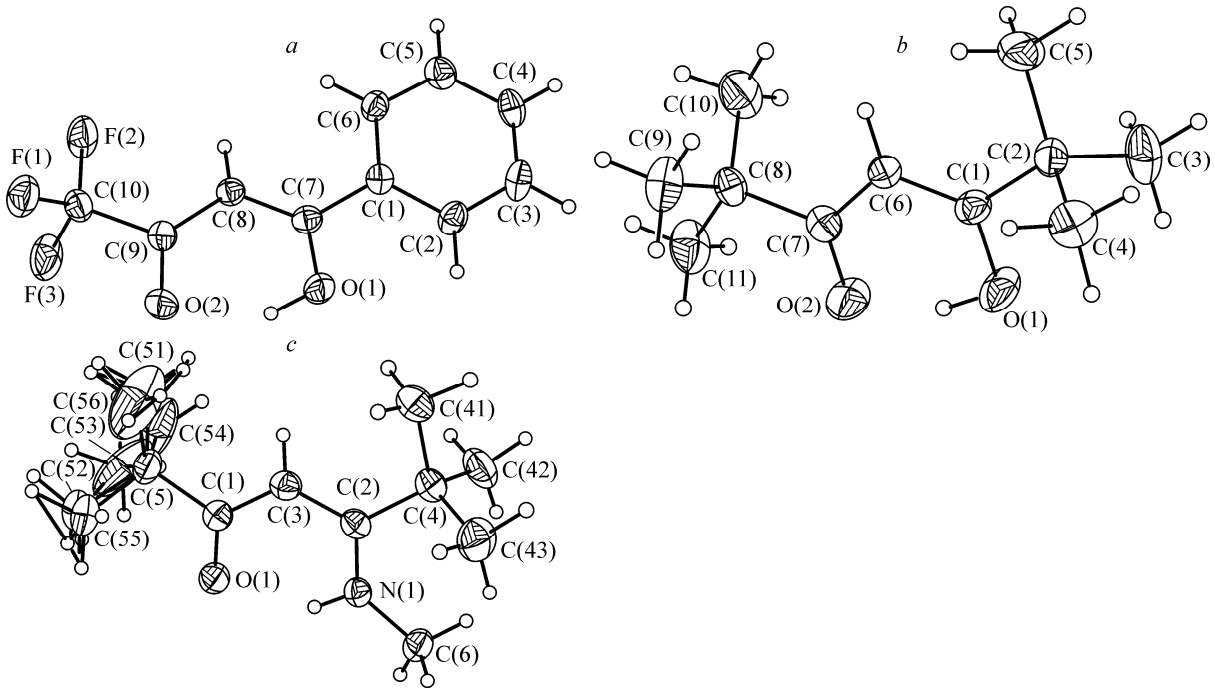

Fig. 2. Structure of Hbtf (**1**) (*a*), Hdpm (**2**) (*b*), and Hmi-dpm (**3**) (*c*) molecules.

DESCRIPTION OF THE CRYSTAL STRUCTURES

The structures of $C_{10}H_7F_3O_2$ (**1**), $C_{11}H_{20}O_2$ (**2**), and $C_{12}H_{23}ON$ (**3**) are built from isolated molecules shown in Fig. 2*a*-*c* respectively. The molecules of ligands **1**, **2,** and **3**, except for the atoms of CF_3 and CH_3 groups, are practically planar within 0.06 Å; in ligand **1,** deviations of atoms of the Ph ring from the rms plane do not exceed 0.01 Å. In the structure of **1,** the ligand molecules are arranged in layers parallel to the [010] direction (Fig. 3*a*), while in the structures of compounds **2** and **3** the molecules follow the parquet motif along the *a* axis (Fig. 3*b* and *c*). In the molecule of ligand **3**, one of the $C(CH_3)_3$ groups is disordered. Bond lengths are similar in ligands **1**, **2**, and **3** (Table 3) and match well to the literature data [11]. Moreover, in the molecules of the ligands there are intramolecular O–H…O (1.735 Å and 1.532 Å for **1** and **2** respectively) and N–H…O (1.904 Å for **3**) hydrogen bonds that form a six-membered planar pseudo- heterocycle (HO_2C_3) in **1** and **2** and (HNC_3O) in **3**. Intermolecular C–H…O contacts (H…O 2.44 Å) can be noted in the structure of ligand **3** (Fig. 3*c*).

QUANTUM CHEMICAL CALCULATIONS

Quantum chemical calculations of Hbtf, Hdpm, Hi-dpm, Hmi-dpm and their sodium complexes have been carried out in order to explain the different reactivity of the ligands in chelate formation. The compounds were calculated at the DFT level of theory, using Becke's three-parameter hybrid functional [12] and the Lee-Yang-Parr correlation functional [13] (B3LYP) implemented in the Jaguar package [14]. Atomic orbitals were described by the 6-31G** basis set. The geometry of the fragments was optimized analytically to a gradient of $5 \cdot 10^{-4}$ au. Selected bond lengths of the optimized Hbtf, Hdpm, Hi-dpm, and Hmi-dpm molecules are given in Table 4. Atomic labeling follows the X-ray crystallography notation. The calculated bond lengths are in good agreement with the experimental values, indicating the applicability of the used quantum chemical approach for this class of compounds. The analysis of the Table 4 data provides evidence that the O(2)–C(9) bond length is almost insensitive to the nature of the substituent in the ring and the adjacent chelating atom (oxygen or nitrogen). The C–N bond is longer than the C–O bond, and the methyl group substitution for the nitrogen hydrogen atom weakens the bond. A successive elongation of the C(7)–C(8) bond in these series of molecules indicates a decrease in the π-electron interactions between these

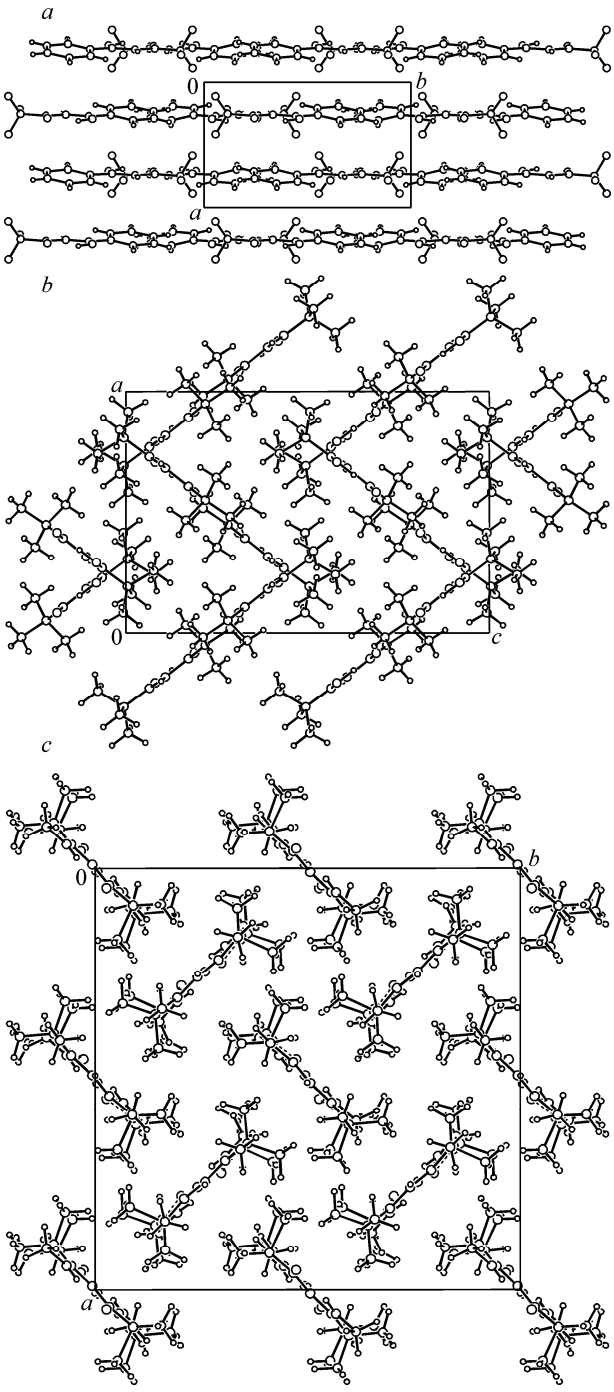

Fig. 3. Molecular packing in the crystals of Hbtf (*a*), Hdpm (*b*), Hmi-dpm (*c*).

atoms when the phenyl moiety is substituted by the *tert*-butyl group, the oxygen atom by nitrogen, and the nitrogen hydrogen atom by the methyl group. Also in these series, the distance between the carbon atom of the chelate ring and the substituent tends to enlarge. The C(9)–C(8) distance between the atoms is practically insensible to these substitutions.

The energy of the complex formation was defined as: $E^{form} = E^{compl} - E^{lig} - E^{Na} + E^{H}$, where E^{compl} and E^{lig} are the total energies of the complex and the ligand; E^{Na} and E^{H} are the energies of the sodium and hydrogen atoms calculated using the same basis set as for the compounds. The obtained values are given in Table 4. The positive energy of the complex formation with sodium indicates the endothermic nature of the process. Therefore, the calculations prove that the complex

TABLE 3. Bond Lengths *d* (Å) for Compounds **1**, **2**, and **3**

Bond	*d*	Bond	*d*	Bond	*d*	Bond	*d*
Compound **1**				Compound **2**			
C(1)–C(2)	1.398(2)	C(8)–C(7)	1.385(2)	O(1)–C(1)	1.327(1)	C(7)–C(6)	1.434(2)
C(1)–C(6)	1.398(2)	C(8)–C(9)	1.406(2)	O(2)–C(7)	1.256(2)	C(7)–C(8)	1.527(2)
C(1)–C(7)	1.470(2)	O(2)–C(9)	1.255(2)	C(1)–C(2)	1.515(2)	C(8)–C(10)	1.526(2)
C(2)–C(3)	1.385(2)	C(9)–C(10)	1.530(2)	C(1)–C(6)	1.365(2)	C(8)–C(11)	1.527(2)
C(3)–C(4)	1.384(2)	F(1)–C(10)	1.331(2)	C(2)–C(3)	1.533(2)	C(8)–C(9)	1.528(2)
C(5)–C(4)	1.390(2)	F(2)–C(10)	1.329(2)	C(2)–C(4)	1.535(2)	O(1)–H(1)	1.00
C(6)–C(5)	1.388(2)	F(3)–C(10)	1.331(2)	C(2)–C(5)	1.521(2)		
O(1)–C(7)	1.315(1)	O(1)–H(1)	0.882				
Bond	*d*	Bond	*d*	Bond	*d*	Bond	*d*
Compound **3**							
O(1)–C(1)	1.253(2)	C(1)–C(5)	1.540(2)	C(4)–C(41)	1.540(3)	C(5)–C(55)	1.475(5)
N(1)–C(2)	1.339(2)	C(2)–C(3)	1.392(2)	C(4)–C(42)	1.543(3)	C(5)–C(51)	1.533(7)
N(1)–C(6)	1.457(2)	C(2)–C(4)	1.538(2)	C(5)–C(53)	1.393(6)	C(5)–C(54)	1.668(6)
N(1)–H(1)	0.84(2)	C(3)–H(3)	0.95(2)	C(5)–C(56)	1.431(13)	C(5)–C(52)	1.669(7)
C(1)–C(3)	1.419(2)	C(4)–C(43)	1.529(3)				

TABLE 4. Bond Lengths (Å) from the B3LYP Calculations of the Molecules and the Interaction Energy of the Ligands with Sodium (eV)

Bond length	Hbtf	Hdpm	Hi-dpm	Hmi-dpm	Bond length	Hbtf	Hdpm	Hi-dpm	Hmi-dpm
O(1)–C(7)	1.318	1.323	—	—	C(7)–C(1)	1.450	1.524	1.539	1.545
O(2)–C(9)	1.256	1.259	1.252	1.256	C(9)–C(10)	1.519	1.542	1.553	1.553
C(7)–C(8)	1.363	1.380	1.385	1.395	N–C(7)	—	—	1.347	1.352
C(9)–C(8)	1.453	1.438	1.440	1.435	E^{form} of the complex	0.41	0.75	1.25	1.57

formation between the ligand and the sodium atom at 0 K is energetically unfavorable. This deficiency should be much smaller under synthetic conditions (temperature ranging from room to 101°C). An increase in the formation energy of the sodium complex in the series of the studied ligands is consistent with the experimental trend. Indeed, as we have found, the formation of the sodium complex is the most rapid with Hbtf; complexation with Hdpm requires more time; the reaction with Hi-dpm occurs only on heating of the reaction mixture to 80°C, and the complex with Hmi-dpm does not form even in boiling dioxane.

MODELING OF THE MOLECULAR STRUCTURE OF Cu(mi-dpm)$_2$

The obtained experimental and theoretical data give evidence that the Hmi-dpm ligand significantly differs from the other three. Therefore, it needs to explain why ligand **3** does not form Na(I) and Cu(II) chelates. For this purpose, based on the available structural data for the molecules of Cu(mi-aa)$_2$ [15] and Cu(i-dpm)$_2$ [8], we tried to model the hypothetical structure of Cu(mi-dpm)$_2$ using the SHELXTL program [9] (Fig. 4*a* and *b)*. The structure of the chelate cores is different in these complexes. In Cu(mi-aa)$_2$, metallocylces make an angle of ~47°, so the nearest environment of the copper atom, including four oxygen and nitrogen atoms, is intermediate between a square and a tetrahedron (Fig. 4*a*). The metallocycles are coplanar in Cu(i-dpm)$_2$, and the nearest environment of the copper atoms is quadratic (Fig. 4*c*). The task for the simulation was the replacement of the terminal CH_3 groups by $(C(CH_3)_3$ groups in the Cu(mi-aa)$_2$ molecule and of the NH

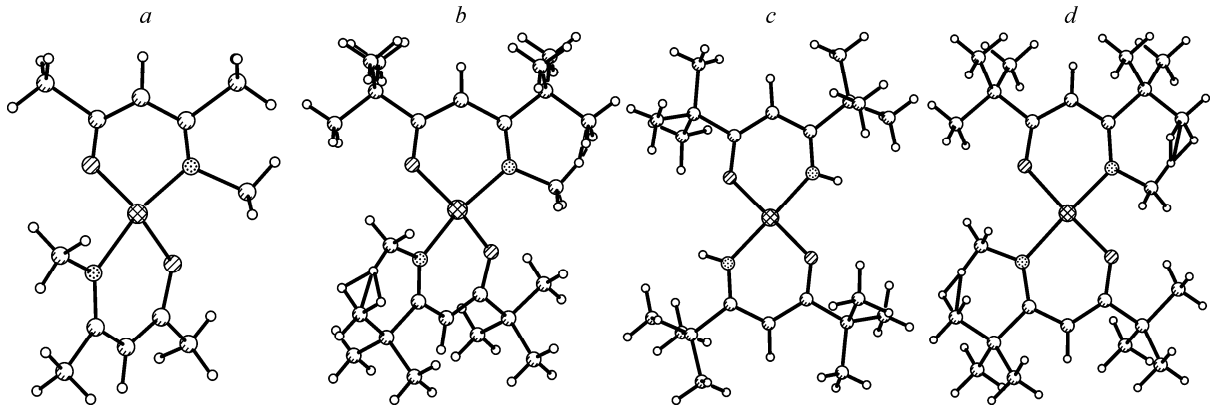

Fig. 4. Experimental structure of the Cu(mi-aa)$_2$ molecule (*a*) and geometrically simulated structure of Cu(mi-dpm)$_2$ (*b*). Experimental structure of the Cu(i-dpm)$_2$ molecule (*c*) and geometrically simulated structure of Cu(i-dpm)$_2$ (*d*).

groups by the NCH_3 groups in the Cu(i-dpm)$_2$ molecule. All hydrogen atoms of the terminal methyl groups in the Cu(mi-aa)$_2$ molecule were removed and geometrically substituted by six C atoms at a distance of 1.54 Å. Then, hydrogen atoms were added to these carbon atoms at a distance of 1.0 Å. In the Cu(i-dpm)$_2$ molecule, two hydrogen atoms at the nitrogen atoms were removed and substituted by C atoms at a distance of 1.45 Å. Hydrogen atoms were added to these carbon atoms at a distance of 1.0 Å. The structures of the Cu(mi-dpm)$_2$ molecule obtained on transformation of the terminal CH_3 groups into ($C(CH_3)_3$ groups in the Cu(mi-aa)$_2$ molecule and on transformation of the NH groups into NCH_3 groups in the Cu(i-dpm)$_2$ molecule are shown in Fig. 4*b* and *d*. Fig. 4 indicates that the formation of metallocycles for Hmi-dpm must be hindered by the intraligand overlap of the substituents.

The simulation has shown that the formation of Hmi-dpm metallocycles with Cu(II) should result in the intraligand overlap of the methyl group atoms at the nitrogen atom and the atoms of one of the methyl groups in the substituent irrespective of the mutual inclination of the metallocycles. In other words, the formation of the metallocycle is sterically hindered for the Hmi-dpm ligand, and, hence, the Cu(mi-dpm)$_2$ complex. Similar sterical reasons are likely to explain a failure in the synthesis of Nami-dpm, in contrast to Naptf, Nadpm, and Nai-dpm in the reaction of metallic sodium with these ligands.

It should be noted that, when this paper was in revision, we succeeded in the preparation of Cu(mi-dpm)$_2$ by the reaction of ligand **3** with $Cu(OCH_3)_2$ in boiling toluene in a stream of dry nitrogen. The complex was purified by sublimation; Cu(mi-dpm)$_2$ is a green-colored compound; *m.p.* 152-153°C.

This study was supported by RFBR grant No. 11-03-00197-a.

REFERENCES

1. B. G. Gribov, G. A. Domrachev, B. V. Zhuk, et al., *Deposition of Films and Coatings by Decomposition of Organometallics* [in Russian], Nauka, Moscow (1981).
2. T. Kodas and M. Hampden-Smith (eds.), *The Chemistry of Metal CVD*, New York–Basel–Cambridge–Tokyo, VCH, Weinhem (1994).
3. R. Boese, M. Yu. Antipin, D. Blaser, and K. A. Lyssenko, *J. Phys. Chem. B*, **102**, 8654-8660 (1998).
4. G. K. Fukin, A. P. Pisarevskii, A. I. Yanovskii, and Yu. T. Struchkov, *Zh. Neorg. Khim.*, **38**., 1205-1211 (1993).
5. J. A. Belot, J. Clark, J. A. Cowan, et al., *J. Phys. Chem. B*, **108**, 6922-6926 (2004).
6. S. Sans-Lenain, A. Reynes, and A. Gleizes, *Acta Crystallogr*., *Cryst. Struct. Commun*., **48**, 1788 (1992).
7. S. Ozturk, M. Akkurt, and S. Ide, *Z. Kristallogr*., **212**, 808 (1997).
8. P. A. Stabnikov, G. I. Zharkova, I. A. Baidina, et al., *Polyhedron*, **26**, 4445-4450 (2007).

9. Bruker AXS Inc. (2004). APEX2 (Version 1.08), SAINT (Version 7.03), SADABS (Version 2.11) and SHELXTL (Version 2008/1). Bruker Advanced X-ray Solutions. Madison, Wisconsin, USA.
10. G. M. Sheldrick, *SHELX97*, *Release 97-2*, Univ. Göttingen, Germany (1998).
11. F. H. Allen, O. Kennard, and D. G. Watson, *J. Chem. Soc*., *Perkin Trans*., S1-S19 (1987).
12. A. D.Becke, *J. Chem. Phys*., **98**, No. 7, 5648-5652 (1993).
13. C. Lee, W. Yang, and R. G. Parr, *Phys. Rev. B*, **37**, No. 2, 785-789 (1988).
14. *Jaguar*, *Version 7.8*, Schrödinger, LLC, New York (2011).
15. I. A. Baidina, P. A. Stabnikov, A. D. Vasiliev, et al., *J. Struct. Chem.,* **45**, No. 4, 671-677 (2004).